Science Bulletin xxx (xxxx) xxx

Contents lists available at ScienceDirect

Science Bulletin

journal homepage: www.elsevier.com/locate/scib

Article

Genetically engineered MSCs overexpressing hepatocyte growth factor for the treatment of human refractory wounds

Min Nie [a,1], Danqing Huang [a,1], Dandan Wang [a], Yuanjin Zhao [a,b,*], Lingyun Sun [a,**]

[a] Department of Rheumatology and Immunology, Nanjing Drum Tower Hospital, Affiliated Hospital of Medical School, Nanjing University, Nanjing 210002, China
[b] School of Biological Science and Medical Engineering, Southeast University, Nanjing 210096, China

ARTICLE INFO

Article history:
Received 2 September 2025
Received in revised form 16 October 2025
Accepted 18 November 2025
Available online xxxx

Keywords:
Mesenchymal stromal cell
HGF
Hydrogel
Refractory wounds
Wound healing

ABSTRACT

Refractory wounds (RWs) are a common and severe complication of many diseases; however, the existing therapeutic methods are unsatisfactory in clinical practice. Here, we observed significant downregulation of the hepatocyte growth factor (HGF) in plasma samples from patients with autoimmune diseases. We used electroporation to deliver a plasmid containing HGF to induce its overexpression on mesenchymal stromal cells (MSC^{HGF}) and loaded them into an injectable hydrogel to treat RWs in patients with clinical autoimmunity. The MSC^{HGF} exhibited stable HGF expression and secretion. In addition, they displayed a self-reinforcing loop, enhanced migration, and improved anti-apoptosis capacity via the autocrine activation of the c-Met-mediated phosphatidylinositol 3-kinase (PI3K)-protein kinase B (AKT) signaling pathway. Furthermore, the HGF (as well as other bioactive factors) secreted from the MSC^{HGF} significantly augmented the migration and angiopoiesis of vascular endothelial cells, decreased the cellular inflammation of macrophages, and improved extracellular matrix remodeling in fibroblasts. According to these features, we demonstrated that the MSC^{HGF}-loaded injectable hydrogel boosted cellular functions and afforded a long-acting healing efficacy in the treatment of clinical autoimmune patients with RWs. Therefore, the genetically engineered MSC^{HGF} and their dispersed hydrogel system will have clinical significance for wound therapy.

1. Introduction

Refractory wounds (RWs) are the most devastating and common complications of uncontrolled diseases, such as metabolic and autoimmune diseases [1–3]. Characterized by vascular wall degeneration necrosis, inflammatory cell infiltration, and tissue ulcerates, RWs tend to cause vascular damage and tissue necrosis, together with resulting physical and mental suffering among the affected individuals [4–7]. Based on the normal mechanism underlying the wound-healing stages (hemostasis, inflammation, proliferation, and remodeling), various therapeutic avenues, including wound-dressing products [8–10], bioengineered skin grafts [11–16], and cell therapies [17–22], have been developed to treat these wounds [23–25]. Although some progress has been reported for simple wounds, few of these therapies exert practical clinical effects on RWs. The cause of these unsatisfactory treatment outcomes can be ascribed to the individual variations observed among patients with different underlying diseases [26]. In particular, systemic autoimmune diseases including systemic lupus erythematosus (SLE), systemic sclerosis (SSc), dermatomyositis (DM), vasculitis (VS), sicca syndrome (SS), and rheumatoid arthritis (RA) disrupt wound healing through overlapping yet distinct pathophysiological mechanisms—creating a "hostile microenvironment" that perpetuates tissue damage and impairs repair—yet the complex wound-healing process coordinated by immune and resident cells remains poorly investigated in these specific autoimmune conditions [27–37]. Thus, effective therapeutic stratagems derived from the molecular mechanisms underlying these diseases for the treatment of their associated RWs treatments remain lacking.

In this study, based on information collected from the plasma samples of patients with clinical autoimmune diseases, including SLE, SSc, SS, RA, VS, and DM, we found significant downregulation of the hepatocyte growth factor (HGF) in patients with SLE with skin lesions. Furthermore, we revealed its underlying molecular mechanism and proposed a novel genetically engineered mesenchymal stromal cell (MSC) therapy for treating RWs in patients

* Corresponding author at: Department of Rheumatology and Immunology, Nanjing Drum Tower Hospital, Affiliated Hospital of Medical School, Nanjing University, Nanjing 210002, China.
** Corresponding author.
E-mail addresses: yjzhao@njglyy.com (Y. Zhao), lingyunsun@nju.edu.cn (L. Sun).
[1] These authors contributed equally to this work.

https://doi.org/10.1016/j.scib.2025.11.046
2095-9273/

with clinical autoimmune diseases, as schematically depicted in Fig. 1. Previous studies have demonstrated that HGF participated in the regulation of cell growth, motility and morphogenesis; however, its role in wound healing in patients with autoimmune disease has not been thoroughly explored [38–40]. Through our research on blood samples from clinical patients, we have discovered that HGF was expressed at low levels among these individuals. By contrast, MSC therapies have afforded the therapeutic effects of ameliorating inflammation and promoting angiopoiesis and new tissue formation [41–45]. Therefore, we hypothesized that using MSCs expressing HGF at high levels promotes cell proliferation and migration by activating the phosphatidylinositol 3-kinase (PI3K)–protein kinase B (AKT) signaling pathway, thus leading to the effective recovery of RWs in patients with SLE, even in those with other autoimmune diseases.

To confirm this hypothesis, we developed *HGF*-genetically engineered MSCs (MSC^{HGF}) through electroporation and loaded them onto a hydrogel to treat patients with autoimmunity and RWs. The constructed MSC^{HGF} exhibited stable HGF expression and secretion, leading to the triggering of the PI3K–AKT signaling pathway via c-Met-mediated autocrine activation. Moreover, to guarantee the survival and retention time of these MSC^{HGF} on RWs surfaces, we also dispersed them into an injectable hyaluronic acid (HA) hydrogel—this design enables sustained, effective therapeutic effects. Notably, HA possesses key properties that make it uniquely suited to address the multifaceted challenges of autoimmune RWs: it originates from the natural extracellular matrix (ECM), exhibits anti-inflammatory activity, supports tissue repair, and has well-established clinical translatability. Based on these features, we demonstrated that significant therapeutic effects could be achieved for clinical RWs in patients with autoimmunity using the MSC^{HGF}-loaded injectable HA hydrogel reported here. These results indicated that our genetically engineered MSC^{HGF} and their dispersed hydrogel have clinical significance for treating RWs and other relative diseases.

2. Materials and methods

2.1. Materials

Lipopolysaccharide (HY-D1056), HGF (HY-P7121), LY294002 (HY-10108), and Puromycin dihydrochloride (HY-B1743A) were purchased from MedChemExpress (Monmouth Junction, NJ, USA). Cell Counting Kit-8 was obtained from Yeasen Biotech (Shanghai, China). Super FastPure Cell RNA Isolation Kit (RC102) was purchased from Vazyme Biotech Co., Ltd. EdU Cell Proliferation Imaging Assay Kit was obtained from Wuhan Fine Biotech Co., Ltd. The apoptosis detection kit was purchased from Abbkine (Wuhan, China). HGF ELISA Kit was purchased from 4A Biotech (Beijing, China). 4,6-diamidino-2-phenylindole (DAPI) was obtained from Elabscience Biotech Co., Ltd. Dulbecco's Modified Eagle Medium: Nutrient Mixture F-12 (DMEM/F-12), fetal bovine serum (FBS), and penicillin/streptomycin (P/S) were purchased from Biosharp Biotechnology. Trypsin-EDTA solution was obtained from BioChannel Biotechnology Co., Ltd. (Nanjing, China). Cell saving regent (CELLSAVING) was obtained from New Cell & Molecular Biotech (NCM, Suzhou, China). Hyaluronic acid gel was purchased from Nanjing Tianzong Yikang Biotechnology Co., Ltd. (Nanjing, China).

2.2. Cell culture and CM collection

Human umbilical vein endothelial cells (HUVECs), the murine-macrophage cell-line RAW264.7, and the mouse fibroblast cell-line NIH 3T3 were purchased from the Shanghai Institute of Cell

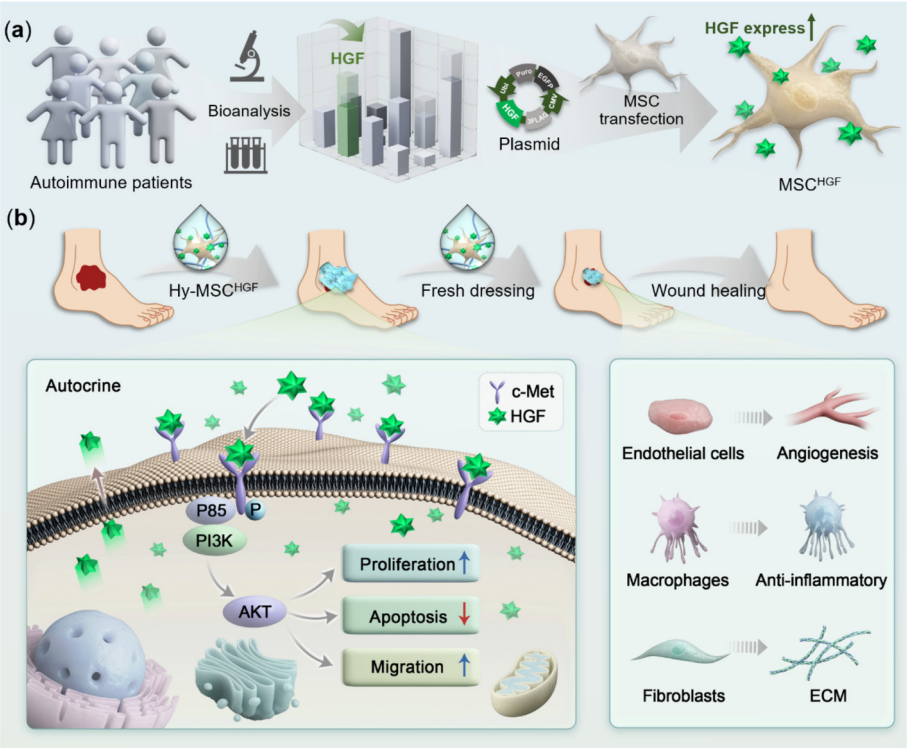

Fig. 1. Schematic illustration of the clinical analysis of autoimmune patients and the establishment of MSC^{HGF} for RWs treatment. (a) By detecting blood samples from clinical autoimmune patients with RWs, we found a significantly decreased HGF level. Based on this, we constructed HGF-highly expressed MSC via electroporation. (b) Combined with biocompatible hydrogel, MSC^{HGF} was applied on clinical autoimmune patients with RWs. Hy-MSC^{HGF} effectively promoted cell proliferation, migration, and inhibited apoptosis through MSC autocrine; meanwhile enhancing angiogenesis, anti-inflammatory, and ECM formation through paracrine, leading to outstanding RWs treating efficacy.

Biology, Chinese Academy of Sciences (Shanghai, China). Human foreskin fibroblasts (HFFs) were a generous gift from Dr Yihe Chen. MSCs were obtained from the Clinical Stem Cell Center of Nanjing Drum Tower Hospital. Recombinant HGF plasmids were transfected into MSCs by electrotransfection and selected by puromycin. After 2 d of culture, conditioned medium (CM) was collected by centrifuging (2500 r/min for 5 min) to remove cell debris.

2.3. Proliferation assay

MSC^{Vector} or MSC^{HGF} cells were cultured on 12-well plates. After pretreated with HGF or CM for 48 h, cells were stained with EdU according to the manufacturer's instruction and results were obtained using confocal microscopy. EdU cell proliferation of HFFs was also performed as described above.

2.4. Wound healing assay

MSC^{Vector} and MSC^{HGF} were plated in a 6-well plate and grew to about 80% confluence, the cell monolayer was scratched using a pipette tip and the cells were subsequently washed twice with PBS followed by incubation with HGF or CM for 24 h. Then, representative photos were taken at indicated times under an optical microscope. Wound healing assay of HUVECs was also followed as described above.

2.5. Anti-apoptosis assay

MSC^{Vector} and MSC^{HGF} were cultured on 6-well plates and pretreated with HGF and CM. Next, MSCs were treated with 5 mmol/L H_2O_2 (Aladdin Bio-chem, Shanghai) for 24 h and stained with annexin V-fluorescein isothiocyanate and propidium iodide (PI) for 30 min before measured using a flow cytometer.

2.6. QRT-PCR and RNA sequencing

Total RNA from cultured cells was extracted using Trizol reagent, and reverse transcription of the RNA was performed using the YfxScript 1st Strand cDNA Synthesis System (Yfxbio Biotech Co., Ltd., Nanjing, China); quantification of the resulting cDNA was then conducted using Universal 2 × SYBR Green Fast qPCR Master Mix. The primer sequences for qRT-PCR are listed in Table S2 (online). For RNA sequencing, 1 μg of total RNA was used per sample, and the assay was performed on MSC^{Vector} and MSC^{HGF} cells by Novogene Co., Ltd. (Beijing, China).

2.7. Western blotting analysis

Cellular proteins were extracted using radioimmune precipitation assay buffer, and Western blot analysis was following established experimental protocols. The following antibodies used for Western blotting—HGF, p-AKT, AKT, and GAPDH were purchased from Zen-bioscience.

2.8. Expression profiling of LPS-induced macrophages

RAW 264.7 cells were seeded in 12-well culture plates and treated with 100 ng/mL LPS. After 6 h of incubation, the LPS-containing supernatants were removed, and the cells were gently washed three times with PBS. The cells were then treated with CM for 24 h. Following CM treatment, immunofluorescence staining was performed to assess the expression profile of macrophages, in accordance with established protocols. The antibodies used for immunofluorescence are listed below: NOS2 (Solarbio), CD68 (Bosterbio), and CD206 (Bioss). Subsequently, the expression of relevant genes in the macrophages was determined by qRT-PCR.

2.9. Tube formation assay

HUVECs were used in tube formation assay. 1×10^4 HUVECs were seeded in 48-well plate with adding 200 μL of Matrigel (KGL5104, KeyGen BioTECH). Following incubation with CM for 24 h, confocal microscope was applied to take images and tube length was quantified by Image J software.

2.10. Mice skin excisional wound healing model

All animal care and handing procedures were approved by the Institutional Animal Care and Use Committee of the Affiliated Drum Tower Hospital of Nanjing University Medical School (ethics number 2020AE02014). The full-thickness skin defect model was established using MRL/lpr mice. After the mice were anesthetized and shaved, a full skin defect wound (0.8 cm in diameter) was formed on the back of each mouse and randomly divided into four groups. Then, the mice were treated in different ways: (1) no treatment was applied (untreated group); (2) treating the wounds with hydrogel (Hydrogel group); (3) treating the wounds with MSC^{Vector}-loaded hydrogel (Hy-MSC^{Vector} group); (4) treating the wounds with MSC^{HGF}-loaded hydrogel (Hy-MSC^{HGF} group). 200 μL MSC-loaded hydrogels were injected through a syringe without syringe needle to cover wounds with full skin defects at a dose of 1×10^6 cells per mL hydrogel. And hydrogels were changed every 48 h in the healing process. A camera was used to record the wound area.

2.11. Histology and immunostaining

Mice were sacrificed at day 8. The skin tissues, including the wound and the surrounding skin were harvested for histology observation. After fixation and paraffin embedding, the specimens were cut into sections with a thickness of 7 mm for standard H&E staining. For the immunohistochemical staining, the tissue slides were prepared following established protocols. The following antibodies were used for immunofluorescence: TNF-α (ABclonal), α-SMA (Proteintech), CD31 (ABclonal), and COL1 (ABclonal), donkey anti-mouse Fluor-568 (ABclonal), donkey anti-Rabbit Fluor-488 (Invitrogen).

2.12. Human refractory wounds treatment

In this clinical trial, patients with RWs refractory to various treatments were enrolled in a compassionate-use program. This study complies with the *Declaration of Helsinki* and was approved by the Human Ethics Committee of Nanjing Drum Tower Hospital (ethics number SC2022-006). Patients screened for this program had to have (i) a diagnosis of autoimmune disease with RWs, (ii) failure to respond to multiple treatments, (iii) the age range from 18 to 80 years and (iv) an understanding of the procedure of cell therapy and agreement to all treatment options. All four patients with RWs (Table S1 online) were recruited at the Department of Rheumatology and Immunology of the Nanjing Drum Tower Hospital. The MSC^{HGF}-loaded hydrogel was prepared by mixing 1×10^6 MSC^{HGF} in 1 mL HA gel. MSC^{HGF}-loaded gel was applied onto the wound bed via a needle-free 1 mL syringe at least twice a week, with dosage adjusted according the wound area. After each application, the wound was covered with medical Vaseline gauze and immobilized with bandages. During dressing changes, the length of the studied wounds was recorded using a numbered scale and wound area was quantified by Image J software.

2.13. Statistical analysis

Quantitative results were presented as means±standard deviation (SD). Statistical comparisons were performed by one-way

analysis of variance (ANOVA) followed by Holm-Sidak tests to compare selected data pairs. Values of $P < 0.05$ were considered statistically significant.

3. Results

3.1. HGF expression in plasma samples from patients with autoimmune disease

In our research, to identify biomarkers of changes among patients with autoimmunity and RWs, we retrospectively investigated their plasma samples. Because HGF is an important cytoprotective factor against injuries and has a range of effects on the events that occur during the wound-healing process, we compared the expression of HGF in plasma samples from clinical autoimmune patients with those from healthy controls using an enzyme-linked immunosorbent assay (ELISA) (Fig. 2a). The results indicated that HGF expression in the samples of patients diagnosed with VS (n = 9; P = 0.2795), SSc (n = 30; P = 0.2356), RA (n = 47; P = 0.9004), and DM (n = 18; P = 0.718) was not significantly different compared with the healthy controls (n = 79) (Fig. 2b–e). However, we found that the level of HGF in patients with SS (n = 43; P = 0.0434) and SLE (n = 111; P = 0.018) was significantly lower (Fig. 2f, g). These results suggest that HGF is involved in the progression of autoimmune diseases and exhibits disease-specific features.

Based on the preliminary statistical results obtained from plasma samples from patients with clinical SLE, we hypothesized that HGF is involved in the development of SLE-associated wound formation. By comparing the HGF levels between patients with SLE with and without skin lesions, we noted a significant downregulation of HGF in the former group (Fig. 2h). These results implied that the decrease in HGF expression observed in patients with SLE might be related to the development of skin lesions. In fact, it is clinically recognized that patients with SLE are prone to developing RWs; however, studies investigating the mechanism and management of this issue are relatively limited. The results reported above indicated that HGF downregulation played an indispensable role in the pathological process of wounds in patients with SLE, which encouraged us to explore its underlying mechanism and therapeutic approaches.

3.2. MSC^{HGF} with higher cell functionalities

According to the findings described above, we hypothesized that the upregulation of HGF at lesion sites is therapeutic by promoting RWs recovery among patients with autoimmunity. Generally, MSCs have been widely used in the biomedical field for their

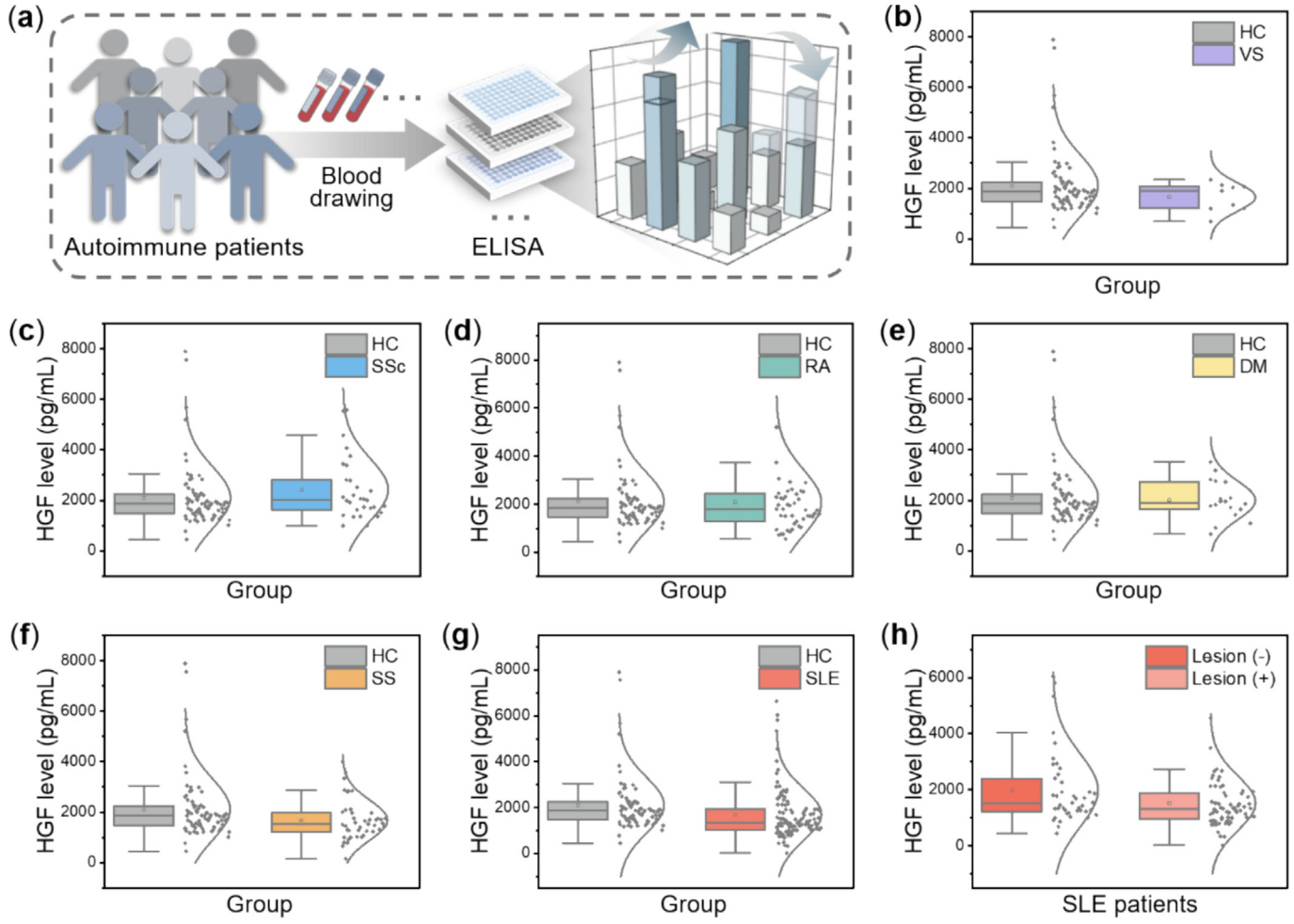

Fig. 2. Analysis of the expression of HGF in plasma samples from autoimmune disease patients. (a) Schematic diagram illustrating the detection of clinical plasma samples from autoimmune disease patients and healthy control individuals by ELISA. (b–g) The expression levels of HGF in VS (b), SSc (c), RA (d), DM (e), SS (f), and SLE (g) plasma samples compared with the healthy controls (HC). (h) The expression levels of HGF in SLE patients with and without skin lesions. (Lesion –: n = 43; Lesion +: n = 68; P = 0.0364)

regenerative capacity, therapeutical potential, and low immunogenicity. In particular, MSC therapy has yielded the practical effects of ameliorating inflammation and promoting angiogenesis, as well as the formation of new tissue. Despite its tremendous success, the limited therapeutic activity of naïve seeding cells severely hampers the clinical practicability of MSC therapy. To address this problem, gene-transfected MSCs have emerged as a feasible avenue. Thus, combined with our clinical findings, we aimed to establish MSCs expressing high levels of HGF to treat RWs in patients with autoimmunity, as illustrated in Fig. 3a.

Considering their biosafety for clinical application, we transferred the recombinant HGF plasmid into MSCs via electroporation. We observed that the morphology of MSC^{HGF} was not different from that of cells carrying the control vector (MSC^{Vector}) (Fig. 3b and Fig. S1a online). In turn, using a flow cytometry analysis, we confirmed that MSC^{HGF} did not exhibit significant differences in MSC surface markers (i.e., CD19, CD34, HLA-DR, CD44, CD90, CD105, and CD73) (Fig. S1b, c online), which indicated that the genetic modification of HGF did not disrupt the typical features of MSCs. Subsequently, it was verified that the HGF expression was significantly increased in MSC^{HGF} compared with MSC^{Vector} (Fig. S2a–c online). Finally, we applied ELISA to investigate HGF secretion. The results confirmed that the MSC^{HGF} secreted about 20 ng of HGF to the conditioned medium within 4 d (Fig. S2d

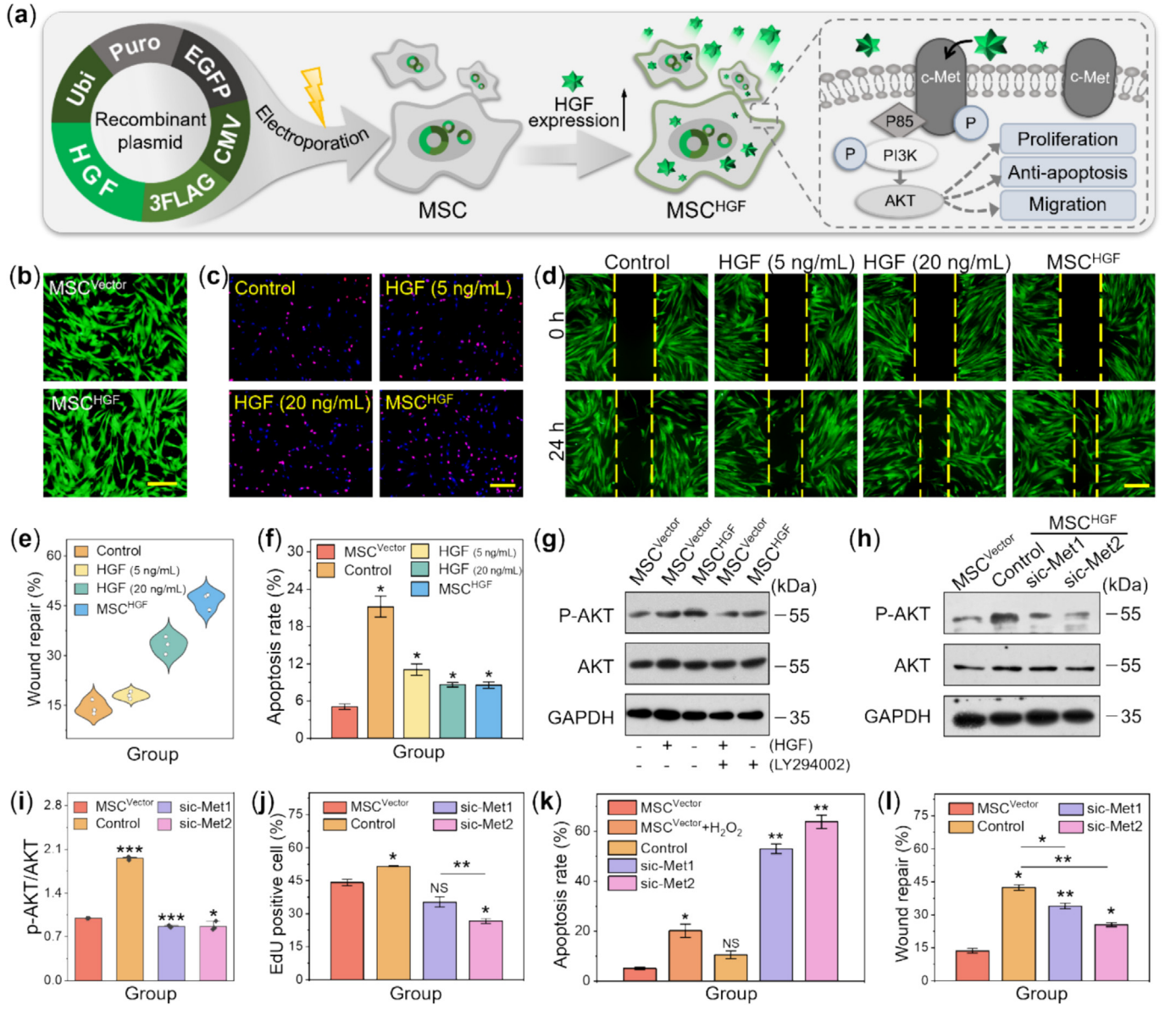

Fig. 3. MSC^{HGF} displayed higher cell proliferation, migration, and anti-apoptosis functionality via c-Met-PI3K-AKT activation. (a) Schematic representation for the construction of MSC^{HGF} and c-Met-mediated autocrine activation of AKT signaling pathway with improved functions of the MSC^{HGF}. (b) Fluorescence microscope images of the constructed MSC^{HGF} and MSC^{Vector}. Scale bar = 100 μm. (c) Representative images from EdU staining of MSC^{HGF} and HGF pretreated MSC^{Vector} from three independent experiments. Scale bar = 150 μm. (d) Representative images from wound healing assay of HGF pretreated MSC^{Vector} and MSC^{HGF} from three independent experiments. Scale bar = 200 μm. (e) Quantified wound healing assay results. (f) Quantified results from apoptosis assay of HGF pretreated MSC^{Vector} and MSC^{HGF} from three independent experiments. (g) p-AKT expression in HGF or LY294002 pre-treated MSC^{Vector} or the MSC^{HGF} tested by Western blotting. (h) Western blotting analysis of indicated protein levels in cell lysates from c-Met-knockdown MSC^{HGF} and MSC^{Vector} cells. (i) The relative levels of p-AKT in cell lysates from c-Met- knockdown MSC^{HGF} and MSC^{Vector} cells. (j–l) Quantified EdU staining (j), apoptosis assay (k) and wound healing assay results (l). $^{*}P < 0.05$, $^{**}P < 0.01$, $^{***}P < 0.001$; NS, not significant.

online), indicating that the recombinant HGF plasmid was successfully transfected into MSCs and that MSC^{HGF} overexpressed HGF effectively.

After the successful establishment of MSC^{HGF}, we attempted to assess the role of autocrine HGF in MSCs. We first examined its effect on cell proliferation *in vitro*. Compared with the control group, MSC^{Vector} pretreated with 5 and 20 ng/mL of free HGF and MSC^{HGF} exhibited observably enhanced proliferation (Fig. 3c and Fig. S3 online). Notably, MSC^{Vector} pretreated with 20 ng/mL of HGF displayed a higher 5-ethynyl-2′-deoxyuridine (EdU)-positive rate than did MSC^{Vector} pretreated with 5 ng/mL of HGF, indicating that HGF can significantly promote MSC proliferation in a concentration-dependent manner. Moreover, a wound-healing assay was performed using MSC^{Vector} pretreated with free HGF and MSC^{HGF}, with the latter exhibiting an increased cell-migratory capability compared with the former (Fig. 3d, e). Furthermore, the MSC^{HGF} and the HGF-pretreated MSC^{Vector} also showed increased resistance to oxidative-stress-induced apoptosis in the presence of 5 mmol/L hydrogen peroxide (H_2O_2) (Fig. 3f and Fig. S4 online). These results indicated that both *HGF* gene modification and free HGF could improve MSC proliferation, migration, and resistance to apoptosis *in vitro*.

To explore the potential mechanisms underlying the improved functionality observed for MSC^{HGF}, RNA sequencing (RNA-seq) analysis was applied to reveal the transcriptome of MSC^{Vector} and MSC^{HGF}. Compared with MSC^{Vector}, 1048 genes were differentially expressed in MSC^{HGF}, of which 477 were upregulated and 571 were downregulated (Fig. S5a online). Moreover, a Kyoto Encyclopedia of Genes and Genomes pathway analysis revealed that those upregulated genes in MSC^{HGF} were enriched for various functions, mainly involving the ECM–receptor interaction, the PI3K–AKT signaling pathway, dilated cardiomyopathy, cell-adhesion molecules, etc. (Fig. S5b online). Given the communication between HGF and c-Met, we hypothesized that the HGF secreted by MSC^{HGF} activates their own PI3K–AKT signaling pathway via autocrine signaling, resulting in the regulation of the function of MSCs. To confirm this hypothesis, we used a PI3K inhibitor (LY294002) to treat MSCs and detected the expression of p-AKT. Western blotting revealed that the expression levels of p-AKT of HGF-pretreated MSC^{Vector} and MSC^{HGF} were higher in the absence of LY294002, whereas they were inhibited in the presence of LY294002 (Fig. 3g and Fig. S6 online). In turn, the expression of AKT was not different between the groups, indicating that the *HGF* gene modification promoted the triggering of the PI3K–AKT signaling pathway in MSC^{HGF}.

To identify the c-Met that was responsible for the HGF-mediated PI3K-AKT signaling pathway triggering in MSCs, we examined the expression of c-Met under different HGF conditions. It was found that the c-Met expression was consistently increased in HGF-pretreated MSC^{Vector} in a concentration-dependent manner (Fig. S7a online). Consistently, the c-Met level was higher in MSC^{HGF} than in MSC^{Vector}, suggesting a potential positive feedback of the HGF-mediated MSC enhancement. In addition, the use of two small interfering RNAs (siRNAs) to knockdown c-Met in MSC^{HGF} (sic-Met1 and sic-Met2) downregulated c-Met expression to 20% of the expression detected in the scrambled control (Fig. S7b online). Moreover, as revealed by Western blotting, the phosphorylation of AKT was greatly reduced in c-Met-knockdown MSC^{HGF} compared with the scrambled control (Fig. 3h, i). Interestingly, this reduction was accompanied by the detection of significantly decreased levels in MSC^{Vector}. Moreover, we further tested the different responses of the c-Met knockdown MSC^{HGF} and the MSC^{Vector} (Fig. 3j–l and Figs. S8–S10 online). The results indicated that the increase in PI3K–AKT pathway activation, cell proliferation, and antiapoptotic and migration effects were all eliminated in the c-Met-knockdown MSC^{HGF}. Taken together, these results demonstrated that the HGF secreted by MSC^{HGF} activated the PI3K–AKT signaling pathway via c-Met-mediated autocrine activation, which led to the increase in self-functionalities and the achievement of self-persistence.

3.3. MSC^{HGF}-modulated wound healing through paracrine effects

Because MSCs play a regulatory role in physiological systems, we investigated the manner in which the secretomes of MSC^{HGF} exerted paracrine effects in wound healing (Fig. 4a). First, we compared RNA expression between MSC^{HGF} and MSC^{Vector}. The analysis of differentially expressed RNAs illustrated the factors that were involved in immune regulation, the inflammatory response, and extracellular structure organization (Fig. S11 online). Moreover, to explore the effects of MSC^{HGF} secretions, CM was separately collected and applied to a secretome proteomics analysis. The results indicated that, compared with MSC^{Vector}, 72 proteins were differentially expressed in MSC^{HGF} ($P < 0.001$), of which 40 were upregulated and 32 were downregulated (Fig. S12 online). Additionally, the gene ontology enrichment analysis suggested that the genes that were upregulated in MSC^{HGF} were enriched for various functional annotations, mainly involving the single-organism cellular process and cytoskeleton organization (Fig. S13 online). Among them, transforming growth factor β (TGF-β) was secreted more abundantly by MSC^{HGF} than by MSC^{Vector}, indicating its possible regulatory role in wound recovery. Additional to the secretomes, HGF could also promote cell migration, cell proliferation, angiogenesis, and synthesis remodeling of the ECM during the wound-healing process. Therefore, we recognized that the secretomes of MSC^{HGF} could reduce the inflammation of macrophages while promoting the migration and angiopoiesis of vascular endothelial cells, as well as improving ECM remodeling in fibroblasts (Fig. 4a).

To examine the function of the secretions of MSC^{HGF} in macrophages, CM was separately collected. Specifically, the RAW 264.7 cells were pretreated with lipopolysaccharide (LPS), and the phenotypes of RAW 264.7 cells were analyzed using immunofluorescence staining for CD68, nitric oxide synthase 2 (NOS2), and CD206. The results showed that, after co-culture with CM, the NOS2 signal decreased, whereas the immunity of CD206 became more pronounced, suggesting the macrophages repolarized from inflammatory to anti-inflammatory type (Fig. 4b, c). Subsequently, the RAW 264.7 cells were pretreated with LPS and the induced inflammatory response was demonstrated through the elevation of interleukin 6 (IL-6), interleukin 1β (IL-1β), and tumor necrosis factor α (TNF-α). These results confirmed that, when the CM from MSC^{Vector} and MSC^{HGF} was added, these inflammatory factors were no longer elevated (Fig. 4g–i). Interestingly, this phenomenon was most obvious for the CM from MSC^{HGF}. Regarding the macrophages-producing anti-inflammatory factors, interleukin 10 (IL-10) and arginase-1 (Arg-1) were upregulated in the MSC^{Vector} CM group and MSC^{HGF} CM group (Fig. 4j, k). Notably, compared with the MSC^{Vector} CM group, the effects of MSC^{HGF} were more potent regarding the promotion of the expression of IL-10 and Arg-1. These results indicated that MSC^{HGF} can modulate macrophage polarization, exert anti-inflammatory activity, and subsequently regulate inflammatory cytokines expression.

The migration and pro-angiogenic function of MSC^{HGF} were also analyzed via wound-healing experiments. By incubating HUVECs in the CM of MSC^{HGF} or MSC^{Vector}, the wound-healing assay revealed that the migratory ability of HUVECs was increased to a greater extent upon treatment with the supernatant from MSC^{HGF} compared with that from MSC^{Vector} (Fig. 4d, l). Consistently, we performed a tube-formation assay using HUVECs. The results indicated that the HUVECs co-cultured with the CM of MSC^{HGF} in a flask covered with Matrigel developed a greater number of tubular structures than did those cultured in the CM of MSC^{Vector} (Fig. 4e). The statistical analysis reported in Fig. 4m also revealed that the

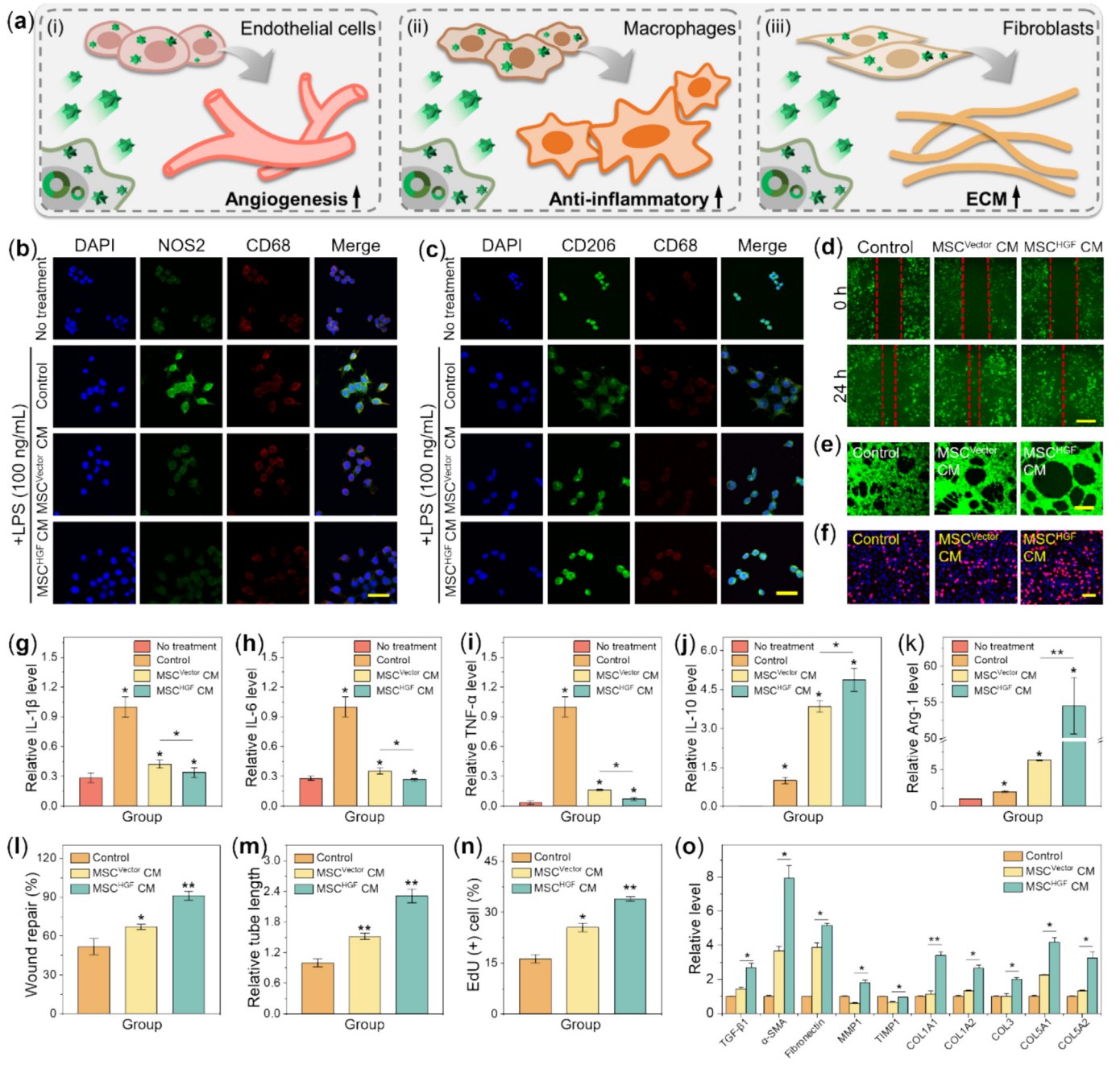

Fig. 4. MSC^{HGF} modulated the wound healing process through paracrine effects. (a) Schematic representation for the secretome preparation, sequencing analysis, and functional characterization of MSC^{HGF}. (b, c) Immunofluorescence staining of CD68 (red), NOS2 and CD206 (green), and nuclei (blue) on macrophages. Scale bar = 50 μm. (d, e) The effects of the MSC^{HGF} on the HUVECs migration (d) and tube formation (e). Scale bar = 200 μm. (f) Representative images from EdU staining of HFFs from three independent experiments. Scale bar = 150 μm. (g–i) The mRNA levels of IL-1β (g), IL-6 (h), and TNF-α (i) in LPS-stimulated RAW 264.7 macrophages. (j, k) The mRNA levels of IL-10 (j) and Arg-1 (k) in LPS-stimulated RAW 264.7 macrophages. (l–n) Quantified wound repair (l), tube length (m) and EdU assay results (n). (o) The mRNA analysis of the selected ECM remolding factors expressed in HFFs treated by MSC^{Vector} and MSC^{HGF} CMs. $^{*}P < 0.05$, $^{**}P < 0.01$; NS, not significant.

total tube length in the MSC^{HGF}-CM-treated group was much higher than that measured in the MSC^{Vector}-CM-treated group, indicating that MSC^{HGF} were able to produce cytokines and growth factors to promote angiogenesis. These results indicated that MSC^{HGF} can exert certain effect on the modulation of HUVEC migration and angiogenesis *in vitro*.

Furthermore, we investigated the proliferative and ECM-remodeling effects of MSC^{HGF} on HFFs. We found that, when HFFs were cultured in the CM of MSC^{HGF}, their proliferation was significantly faster than that of those cultured in the CM of MSC^{Vector} (Fig. S14 online). To confirm the biological effect of MSC^{HGF} on HFFs, EdU detection was performed. Consistent with the CCK-8 assay results, the number of HFFs cultured in the CM of MSC^{HGF} in the proliferation period was greater than that of cells that were co-cultured in the CM of MSC^{Vector} (Fig. 4f, n). These results implied that the CM of MSC^{HGF} enhanced the proliferation of HFFs.

As the synthesis and deposition of ECM are a critical feature in the recovery of chronic wounds, we examined the role of MSC^{HGF} in ECM remodeling. We found that TGF-β was secreted more abundantly in MSC^{HGF}, and that the secreted TGF-β acted as a powerful activator for stimulating fibroblasts to produce ECM components, such as collagen, fibronectin, and matrix metalloproteases (MMPs).

This indicates the certain regulatory role of MSC^{HGF} in wound healing. In addition, by culturing HFFs in the CM of MSC^{HGF} and MSC^{Vector}, several factors, including TGF-β, α–SMA, fibronectin, MMP1, TIMP1, Col1A, Col3A, Col5A1, and Col5A2, were also assessed by qRT-PCR. The results demonstrated that the expression levels of these factors were significantly elevated in cells cultured with the MSC^{HGF} CM group compared with the MSC^{Vector} CM group (Fig. 4o). Therefore, these results suggested that MSC^{HGF} can modulate HFF proliferation and remodel ECM *in vitro*. Taken together, the results reported above demonstrated that the secretomes of MSC^{HGF} could modulate the function of resident cells during wound healing via paracrine effects.

3.4. MSC^{HGF}-laden hydrogel ameliorated wound healing

Leveraging on the above-mentioned verified functionalities of MSC^{HGF}, we further explored the applicability of MSC^{HGF} for treating wounds. As previous studies have demonstrated that hydrogels can be applied as injectable cell-loading vehicles to promote the survival of MSCs and augment therapeutic efficacy *in vivo* [46], we loaded MSC^{HGF} into HA hydrogel to strengthen their therapeutic benefit. Before *in vivo* experiments, we confirmed the injectability, biosafety, and degradation features of HA hydrogel (Figs. S15–S21 online). Furthermore, the tumorigenicity of MSC^{HGF} was also examined. By subcutaneously injecting MSC^{HGF} into the axilla of nude mice for 21 d, we observed that MSC^{HGF} did not induce tumor formation (Fig. S22 online). Therefore, the MSC^{HGF}-laden hydrogel promises to be valuable for wound healing applications.

To test the wound-healing function of the MSC^{HGF}-laden hydrogel *in vivo*, a chronic hard-to-heal SLE wound model was employed, as represented schematically in Fig. 5a. A full-thickness defect wound of about 0.8 cm in diameter was established on the dorsal side of the mice, and the hydrogel, MSC^{Vector}-laden hydrogel (Hy-MSC^{Vector}), and MSC^{HGF}-laden hydrogel (Hy-MSC^{HGF}) were injected, respectively, onto the skin flap immediately after wounding; by contrast, in the negative control (Untreated), no treatment was applied. The results were illustrated in gross images of wounds at different time points during the wound-healing process over 8 d (Fig. 5b). Compared with the untreated group, the wounds in the Hy-MSC^{Vector} and Hy-MSC^{HGF} groups exhibited a better healing appearance, with the Hy-MSC^{HGF} group showing the fastest healing rate. In fact, at the very early healing stage (day 2), although Hy-MSC^{HGF} exhibited a higher healing rate, no discrepancy was found between the Hy-MSC^{Vector} and Hy-MSC^{HGF} groups. Subsequently, the Hy-MSC^{HGF} group displayed the highest wound-closure rate compared with the remaining three groups from day 4. Furthermore, we performed hematoxylin–eosin (H&E) and Masson staining in wound samples to evaluate the histological status during the 8-day period (Fig. 5d and Fig. S23 online). The results confirmed the clear presence of thick and abundant granulation tissue in Hy-MSC^{HGF}-treated wounds, which was much better than that detected in the remaining groups. Taken together, these histological results indicated that Hy-MSC^{HGF} was very suitable for the treatment of SLE wounds, which promoted the formation of the granulation tissue in the wounds, and finally accelerated the healing process.

Based on the desirable anti-inflammatory, angiogenic, and ECM-remodeling performances of MSC^{HGF}, we examined the expression of TNF-α, which is an important biomarker associated with inflammation. The corresponding immunofluorescence staining results revealed that the smallest amount of TNF-α secretion in the regenerated granulation tissue was observed in the Hy-MSC^{HGF} group, thereby demonstrating the alleviated inflammatory states (Fig. 5c, e). In addition, CD31 and α-SMA staining in wound samples was performed to investigate whether the angiogenic response could be activated during the wound-healing process. The results showed that the number of blood vessels detected in the Hy-MSC^{HGF} group was more than that in the Hy-MSC^{Vector} group, whereas the untreated and hydrogel groups displayed modest positive staining (Fig. 5c, f, g). As synthesis of ECM components, especially collagen, is necessary to seal the wounds, the immunostaining results for collagen I (COL1) are also reported. The findings revealed a significantly strong positive staining for COL1 in the Hy-MSC^{HGF} group (Fig. 5c, h). In turn, the untreated group exhibited the weakest positive staining compared with the remaining groups. These results indicated that Hy-MSC^{HGF} can efficiently suppress the inflammatory response, activate the angiogenesis process, and promote collagen synthesis during the wound-healing period.

3.5. MSC^{HGF}-laden hydrogel cured human RWs in clinical settings

Based on the excellent wound-healing capability of the MSC^{HGF}-laden hydrogel observed in mice with SLE, we next evaluated its practical value in patients with RWs and autoimmune conditions, including SLE, gout, vasculitis, and SSc (Fig. 6a). In this clinical trial, four patients (two women and two men) with RWs refractory to several treatments were enrolled in a compassionate-use program. The MSC^{HGF}-loaded hydrogel was applied onto the wound bed, followed by the placement of a medical Vaseline gauze piece cover and bandage immobilization at least twice a week. During the dressing changes, the length of the studied wounds was recorded using a numbered scale. A typical patient in this setting was a woman in her 30s with SLE. Multiple ulcers were found on the patient's leg, one of which did not heal over a long period, even after the administration of various treatments at multiple hospitals. The wound was measured at 1 cm × 1 cm, with a depth of 3.5 cm, and was producing a serous exudate. With the patient's consent, the MSC^{HGF}-loaded hydrogel was introduced into the treatment regimen 1 week after debridement. The results of this procedure showed that, after 37 d of consecutive application of the MSC^{HGF}-loaded hydrogel, the wound was completely healed (Fig. 6b, d). The patient was very satisfied with the outcome of the MSC^{HGF}-loaded hydrogel treatment and thought our method much comfortable than previously received methods.

In addition to the above-mentioned positive treatment outcome and facts, currently, as the number of patients with RWs caused by aging and underlying diseases increases, we look forward to further application of the MSC^{HGF}-loaded hydrogel to other types of RWs, including, but not limited to, those of patients with SLE. At our suggestion and with the patient's consent, a man in his 70s with a 30-year history of gout and hypertension was enrolled in our clinical trial. He had a serious ulcer on his foot that had developed over a period of more than 8 years and negatively impacted his quality of life. At first, he self-treated the wound, but it did not heal completely. He then sought care at the local hospital, undergoing a variety of primary wound dressings and skin grafts, all of which yielded poor results and frequent relapses. When the patient was admitted to our hospital, the wound on his foot was approximately 9 cm × 6 cm in size, with a deep margin and a shallow middle, accompanied by a large amount of exudate. Upon consultation with the patient, our MSC^{HGF}-loaded hydrogel was applied. After several applications of the hydrogel, the exudation of the patient's wound was significantly reduced, epithelial granulation was prompted, and the wound area was gradually reduced (Fig. 6c, e). After 2 months of consecutive application of the MSC^{HGF}-loaded hydrogel, the patient no longer has difficulties with daily living and was extremely pleased with the outcome, as the wound was completely healed without forming a scar (Fig. S25 online).

Encouraged by the unexpected outcomes of the demonstrations described above, two additional patients were recruited into the

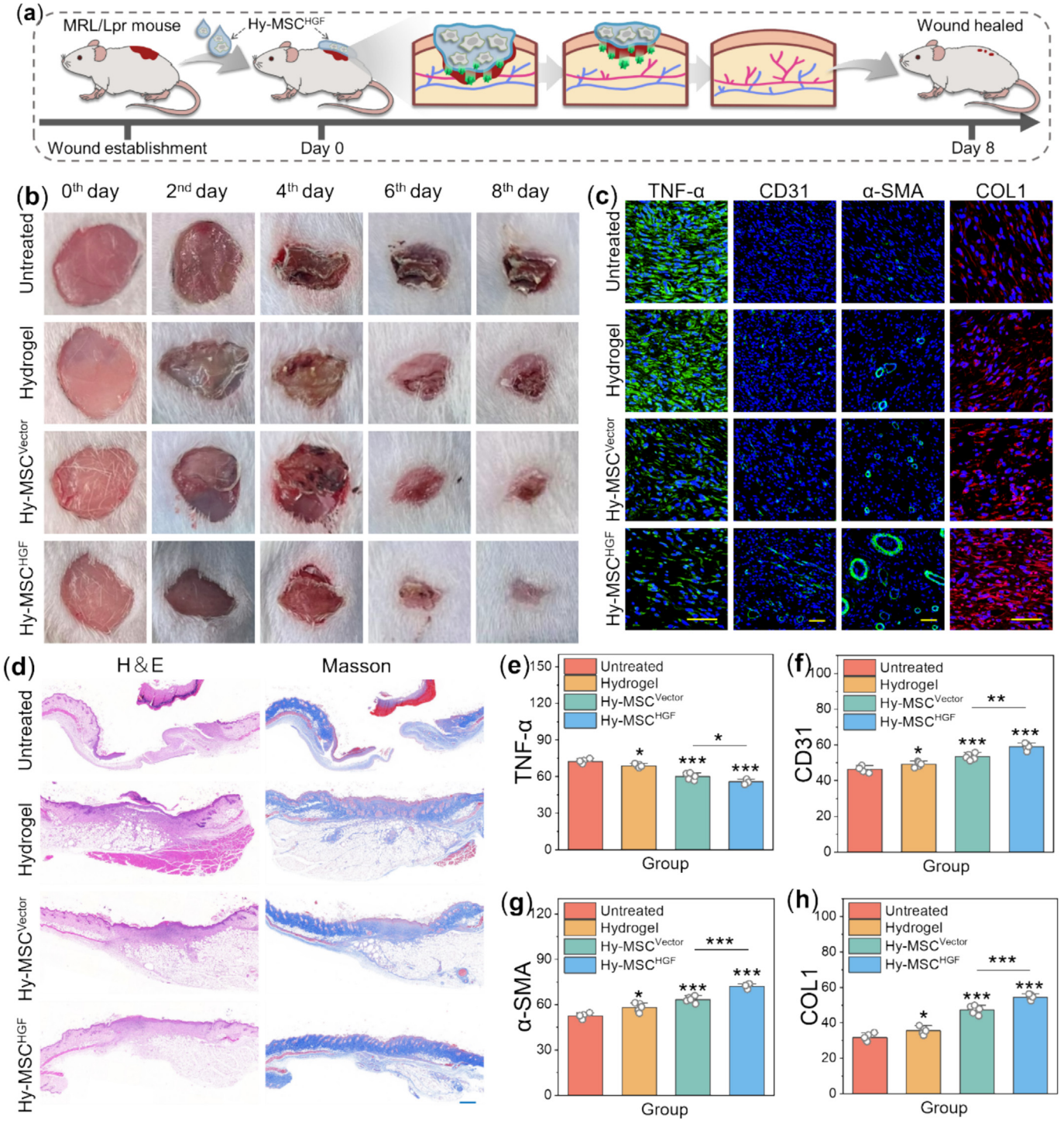

Fig. 5. MSC^{HGF}-laden injectable hydrogel for chronic wound healing. (a) Schematic representation and timeline of application of MSC^{HGF}-laden injectable hydrogel. (b) Representative photos of the skin wounds in untreated, hydrogel, Hy-MSC^{Vector} and Hy-MSC^{HGF} groups. (c) Immunostaining of TNF-α, CD31, α-SMA, and COL1 in granulation tissues after 8 d. Scale bar = 50 μm. (d) H&E and Masson staining of wounds after 8 days at low magnification. Scale bar = 500 μm. Statistical analysis of the mean gray value of TNF-α (e), CD31 (f), α-SMA (g), and COL1 (h) from each group. $^{*}P < 0.05$, $^{**}P < 0.01$, $^{***}P < 0.001$; NS, not significant.

trial and received the MSC^{HGF}-loaded hydrogel treatment. The next patient was a woman in her 30s with vasculitis. She had several ulcers on her feet and had experienced distress and anxiety because of unbearable pain and discomfort. She consented to our MSC^{HGF}-loaded hydrogel treatment as she was desirous of a good outcome. After 37 d of treatment with the MSC^{HGF}-loaded hydrogel, the depth and size of the hole on her feet were decreased (Fig. 6f and Fig. S26 online). Notably, the patient reported a significant reduction in pain during the MSC^{HGF}-loaded hydrogel treatment compared with all of the treatments that she had previously received. We followed up this patient after discharge, with reports of an excellent prognosis and no additional wounds or pain.

The fourth patient was a man in his 60s with SSc and non-healing wounds located over his ankle for several years. After the second application of the MSC^{HGF}-loaded hydrogel, the slough was removed, and the residual wound bed was covered with granulation tissue. In particular, after 1.5 months of this treatment, the

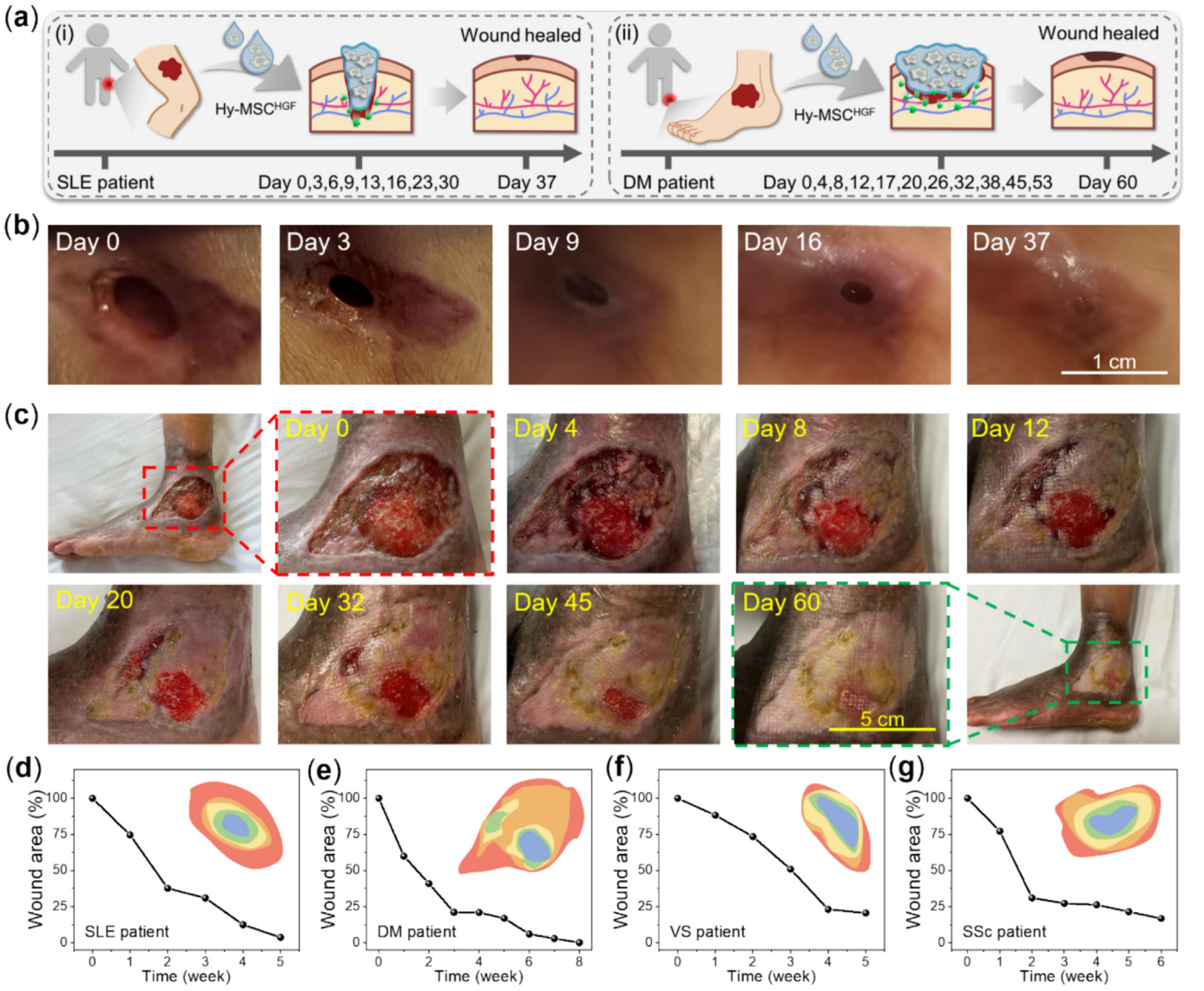

Fig. 6. MSC^{HGF}-laden hydrogel cured human RWs in clinical. (a) Schematic representation and timeline of application of MSC^{HGF}-laden hydrogel for clinical RWs treatment. (i) SLE patient. (ii) Gout patient. (b, c) The wound healing process of the SLE patient (b) and gout patient (c) based on the wound size reduction during the MSC^{HGF}-loaded hydrogel treatment. (d–g) Mean wound area of the wounds in SLE (d), gout (e), vasculitis (f) and SSc (g) patients.

wound was almost healed, and the peri-wound maceration had also improved (Fig. 6g and Fig. S27 online). The patient found our treatment tolerable and atraumatic. He was confident about going out. Therefore, his quality of life improved. According to the positive outcomes and feedback from clinical patients, we believe that our MSC^{HGF}-loaded hydrogel could be used by a range of patients with RWs.

4. Discussion and conclusion

In summary, by analyzing plasma samples of patients with clinical autoimmunity, we found that HGF was involved in the progression of autoimmune diseases and related to the development of skin lesions. These findings inspired us to develop a novel MSC^{HGF}-laden hydrogel for the treatment of clinical RWs. MSC^{HGF} were obtained by transferring a recombinant HGF plasmid into MSCs via electroporation. We demonstrated that MSC^{HGF} played a variety of physiological roles though autocrine and paracrine routes. In terms of autocrine effects, HGF activated the PI3K–AKT signaling pathway via c-Met-mediated autocrine activation, potentially promoting the proliferation, migration, and anti-apoptosis of MSCs. In addition to HGF secretion, we confirmed that the other secretomes of MSC^{HGF} could also reduce the inflammation of macrophages, promote the migration and angiopoiesis of vascular endothelial cells, and improve ECM remodeling in fibroblasts. To implement the practical application of these MSC^{HGF} on wound dressing, we encapsulated them into a biocompatible and injectable hydrogel to increase their survival and retention time. We demonstrated that the MSC^{HGF}-laden hydrogel efficiently inhibited the inflammatory response, activated the angiogenesis process, promoted granulation tissue formation and collagen deposition during the wound recovery in both mouse model and clinical patients with RWs. These features indicated that our MSC^{HGF}-laden hydrogel was efficient and versatile in treating RWs.

Despite the excellent therapeutic efficacy of the MSC^{HGF}-laden hydrogel in clinical patients with RWs, several challenges remain regarding their wide clinical applications. Generally, wound healing includes multiple processes, each of which requires rigorous temporal and spatial regulation [47,48]. Although previous studies have confirmed the contribution of multiple cytokines

and signaling pathways during wound healing, there remains a need to expound the molecular mechanism of interaction between several related factors [49]. Based on this deeper research, new cell therapies with the advantages of good biocompatibility, easy preparation, and controllable release to synchronize the complex process of wound healing are anticipated. In addition, because of individual differences among patients with skin lesions, which might affect the therapeutic effect, it is critical to optimize the loading system [50]. In fact, to improve skin repair and regeneration in patients with different underlying diseases, it is feasible to use an individualized approach with differential factors or drug-delivery systems. Furthermore, wound healing is a complicated dynamic process that includes the participation of many types of histiocytes, thus, the loading of different types of cells according to their engagement would also accelerate healing. However, among the current options for the treatment of RWs, our MSC^{HGF}-laden hydrogel still has great feasibility and therapeutic advantages.

Other than mechanistic and technical aspects, there is still a long way to go in the clinical promotion of engineered cells. Although our cell-loaded system can be used in wound healing or regenerative medicine, more attention is needed to address its long-term effects, such as cell proliferation or permanent engrafting in the host. Of note, at the biotechnology level, bioengineering techniques could be used to render MSCs safe and controllable by endowing them with multiple chemoattractant receptors and other molecules that mediate their homing to inflamed and diseased tissues [42,51–53]. Moreover, products derived from MSCs, such as exosomes or extracellular vesicles, have shown a therapeutic potential similar to that of MSCs [54–56]. In turn, enucleated cells have the property of retaining organelles for energy and protein production, and these cell-free products may be interesting in clinics [57]. In conclusion, by integrating engineered MSCs into clinical centers, research institutes, or companies, we believe that they will benefit a greater number of patients.

Conflict of interest

The authors declare that they have no conflict of interest.

Acknowledgments

This work was supported by the National Key R&D Program of China (2020YFA0710800 and 2020YFA0908200), the National Natural Science Foundation of China (T2225003, 82330055, U24A20380, and 824B2049), the Key Projects of the Jiangsu Basic Research Program (BK20243061), Jiangsu Province Health Department Foundation (H2023087), Jiangsu Province's Major Project in Research and Development (BE2021689), Bethune Charitable Foundation (BCF-QYWL-FS-2024-3), and the Clinical Trials from Nanjing Drum Tower Hospital (2022-LCYJ-ZD-01 and 2025-LCYJ-PY-14).

Author contributions

Yuanjin Zhao and Lingyu Sun conceptualized the idea and structured the article. Min Nie, Danqing Huang, and Dandan Wang conducted literature reviews and composed the manuscript. Min Nie and Danqing Huang contributed to the writing process. Yuanjin Zhao and Lingyun Sun oversaw the manuscript.

Appendix A. Supplementary material

Supplementary data to this article can be found online at https://doi.org/10.1016/j.scib.2025.11.046.

References

[1] GBD 2021 Diabetes Collaborators. Global, regional, and national burden of diabetes from 1990 to 2021, with projections of prevalence to 2050: a systematic analysis for the global burden of disease study 2021. Lancet 2023;402:203–34.
[2] Armstrong DG, Tan T-W, Boulton AJM, et al. Diabetic foot ulcers. JAMA 2023;330:62–75.
[3] Falanga V, Isseroff RR, Soulika AM, et al. Chronic wounds. Nat Rev Dis Primers 2022;8:50.
[4] Talbott HE, Mascharak S, Griffin M, et al. Wound healing, fibroblast heterogeneity, and fibrosis. Cell Stem Cell 2022;29:1161–80.
[5] Jeschke MG, Wood FM, Middelkoop E, et al. Scars. Nat Rev Dis Primers 2023;9:64.
[6] Kanchanawong P, Calderwood DA. Organization, dynamics and mechanoregulation of integrin-mediated cell-ECM adhesions. Nat Rev Mol Cell Biol 2023;24:142–61.
[7] Raffetto JD, Ligi D, Maniscalco R, et al. Why venous leg ulcers have difficulty healing: overview on pathophysiology, clinical consequences, and treatment. J Clin Med 2021;10.
[8] Mookherjee N, Anderson MA, Haagsman HP, et al. Antimicrobial host defence peptides: functions and clinical potential. Nat Rev Drug Discov 2020;19:311–32.
[9] Hua Y, Wang K, Huo Y, et al. Four-dimensional hydrogel dressing adaptable to the urethral microenvironment for scarless urethral reconstruction. Nat Commun 2023;14:7632.
[10] Freedman BR, Hwang C, Talbot S, et al. Breakthrough treatments for accelerated wound healing. Sci Adv 2023;9:eade7007.
[11] Gelain F, Luo Z, Zhang S. Self-Assembling Peptide EAK16 and RADA16 nanofiber scaffold hydrogel. Chem Rev 2020;120:13434–60.
[12] Mao X, Cheng R, Zhang H, et al. Self-healing and injectable hydrogel for matching skin flap regeneration. Adv Sci 2019;6:1801555.
[13] Zhang YS, Khademhosseini A. Advances in engineering hydrogels. Science 2017;356:eaaf3627.
[14] Kharaziha M, Baidya A, Annabi N. Rational design of immunomodulatory hydrogels for chronic wound healing. Adv Mater 2021;33:e2100176.
[15] Zhang J, Zheng Y, Lee J, et al. A pulsatile release platform based on photo-induced imine-crosslinking hydrogel promotes scarless wound healing. Nat Commun 2021;12:1671.
[16] MacNeil S. Progress and opportunities for tissue-engineered skin. Nature 2007;445:874–80.
[17] John JV, Sharma NS, Tang G, et al. Nanofiber aerogels with precision macrochannels and LL-37-mimic peptides synergistically promote diabetic wound healing. Adv Funct Mater 2023;33:2206936.
[18] Gur C, Wang S-Y, Sheban F, et al. LGR5 expressing skin fibroblasts define a major cellular hub perturbed in scleroderma. Cell 2022;185:1373–88.
[19] Maschalidi S, Mehrotra P, Keçeli BN, et al. Targeting SLC7A11 improves efferocytosis by dendritic cells and wound healing in diabetes. Nature 2022;606:776–84.
[20] Vernerey FJ, Lalitha Sridhar S, Muralidharan A, et al. Mechanics of 3D cell-hydrogel interactions: experiments, models, and mechanisms. Chem Rev 2021;121:11085–148.
[21] Harris-Tryon TA, Grice EA. Microbiota and maintenance of skin barrier function. Science 2022;376:940–5.
[22] Mascharak S, des Jardins-Park HE, Davitt MF, et al. Preventing Engrailed-1 activation in fibroblasts yields wound regeneration without scarring. Science 2021;372:eaba2374.
[23] Guo B, Dong R, Liang Y, et al. Haemostatic materials for wound healing applications. Nat Rev Chem 2021;5:773–91.
[24] Caves E, Horsley V. Reindeer light the way to scarless wound healing. Cell 2022;185:4675–7.
[25] Willenborg S, Sanin DE, Jais A, et al. Mitochondrial metabolism coordinates stage-specific repair processes in macrophages during wound healing. Cell Metab 2021;33:2398–12241.
[26] Frykberg RG, Franks PJ, Edmonds M, et al. A Multinational, multicenter, randomized, double-blinded, placebo-controlled trial to evaluate the efficacy of cyclical topical wound oxygen (TWO2) therapy in the treatment of chronic diabetic foot ulcers: the TWO2 study. Diabetes Care 2020;43:616–24.
[27] Sutherland TE, Dyer DP, Allen JE. The extracellular matrix and the immune system: a mutually dependent relationship. Science 2023;379:eabp8964.
[28] Massagué J, Sheppard D. TGF-β signaling in health and disease. Cell 2023;186:4007–37.
[29] Denton CP, Khanna D. Systemic sclerosis. Lancet 2017;390:1685–99.
[30] Sinha S, Sparks HD, Labit E, et al. Fibroblast inflammatory priming determines regenerative versus fibrotic skin repair in reindeer. Cell 2022;185:4717–36.
[31] Konieczny P, Xing Y, Sidhu I, et al. Interleukin-17 governs hypoxic adaptation of injured epithelium. Science 2022;377:eabg9302.
[32] Dekoninck S, Blanpain C. Stem cell dynamics, migration and plasticity during wound healing. Nat Cell Biol 2019;21:18–24.
[33] Klose CSN, Artis D. Innate lymphoid cells as regulators of immunity, inflammation and tissue homeostasis. Nat Immunol 2016;17:765–74.
[34] Nolte M, Margadant C. Controlling immunity and inflammation through integrin-dependent regulation of TGF-β. Trends Cell Biol 2020;30:49–59.
[35] Delacher M, Simon M, Sanderink L, et al. Single-cell chromatin accessibility landscape identifies tissue repair program in human regulatory T cells. Immunity 2021;54:702–20.

[36] Xu L, Shao Z, Fang X, et al. Exploring precision treatments in immune-mediated inflammatory diseases: harnessing the infinite potential of nucleic acid delivery. Exploration 2024;5:20230165.
[37] Zhao Z, Xiong H, Wu J, et al. Targeted ruthenium-based anti-inflammatory nanoagent for enhanced rheumatoid arthritis treatment. Exploration 2025;5:20240043.
[38] Raj S, Kesari KK, Kumar A, et al. Molecular mechanism(s) of regulation(s) of c-MET/HGF signaling in head and neck cancer. Mol Cancer 2022;21:31.
[39] Uchikawa E, Chen Z, Xiao G-Y, et al. Structural basis of the activation of c-MET receptor. Nat Commun 2021;12:4074.
[40] Bradley CA, Salto-Tellez M, Laurent-Puig P, et al. Targeting c-MET in gastrointestinal tumours: rationale, opportunities and challenges. Nat Rev Clin Oncol 2017;14:562–76.
[41] Barrère-Lemaire S, Vincent A, Jorgensen C, et al. Mesenchymal stromal cells for improvement of cardiac function following acute myocardial infarction: a matter of timing. Physiol Rev 2024;104:659–725.
[42] Soliman H, Theret M, Scott W, et al. Multipotent stromal cells: one name, multiple identities. Cell Stem Cell 2021;28:1690–707.
[43] Wang Y, Fang J, Liu B, et al. Reciprocal regulation of mesenchymal stem cells and immune responses. Cell Stem Cell 2022;29:1515–30.
[44] Witwer KW, Van Balkom BWM, Bruno S, et al. Defining mesenchymal stromal cell (MSC)-derived small extracellular vesicles for therapeutic applications. J Extracell Vesicles 2019;8:1609206.
[45] Zhou T, Yuan Z, Weng J, et al. Challenges and advances in clinical applications of mesenchymal stromal cells. J Hematol Oncol 2021;14:24.
[46] Nie M, Kong B, Chen G, et al. MSCs-laden injectable self-healing hydrogel for systemic sclerosis treatment. Bioact Mater 2022;17:369–78.
[47] Naik S, Larsen SB, Cowley CJ, et al. Two to Tango: dialog between immunity and stem cells in health and disease. Cell 2018;175:908–20.
[48] Hu KH, Kuhn NF, Courau T, et al. Transcriptional space-time mapping identifies concerted immune and stromal cell patterns and gene programs in wound healing and cancer. Cell Stem Cell 2023;30:885–903.
[49] Brazil JC, Quiros M, Nusrat A, et al. Innate immune cell-epithelial crosstalk during wound repair. J Clin Invest 2019;129:2983–93.
[50] Ruan H, Li Y, Wang C, et al. Click chemistry extracellular vesicle/peptide/chemokine nanocarriers for treating central nervous system injuries. Acta Pharm Sin B 2023;13:2202–18.
[51] Sui B-D, Zheng C-X, Li M, et al. Epigenetic regulation of mesenchymal stem cell homeostasis. Trends Cell Biol 2020;30:97–116.
[52] Shelby H, Shelby T, Wernig M. Somatic lineage reprogramming. Cold Spring Harb Perspect Biol 2022;14:a040808.
[53] Hoang DM, Pham PT, Bach TQ, et al. Stem cell-based therapy for human diseases. Signal Transduct Target Ther 2022;7:272.
[54] Psaraki A, Ntari L, Karakostas C, et al. Extracellular vesicles derived from mesenchymal stem/stromal cells: the regenerative impact in liver diseases. Hepatology 2022;75:1590–603.
[55] Lin Z, Wu Y, Xu Y, et al. Mesenchymal stem cell-derived exosomes in cancer therapy resistance: recent advances and therapeutic potential. Mol Cancer 2022;21:179.
[56] Ding J-Y, Chen M-J, Wu L-F, et al. Mesenchymal stem cell-derived extracellular vesicles in skin wound healing: roles, opportunities and challenges. Mil Med Res 2023;10:36.
[57] Wang H, Alarcón CN, Liu B, et al. Genetically engineered and enucleated human mesenchymal stromal cells for the targeted delivery of therapeutics to diseased tissue. Nat Biomed Eng 2022;6:882–97.